Catalysis Letters
https://doi.org/10.1007/s10562-019-02929-x

A Highly Active, Recyclable and Cost-Effective Magnetic Nanoparticles Supported Copper Catalyst for N-arylation Reaction

Razieh Zahedi[1] · **Zahra Asadi**[1] · **Fahimeh Dehghani Firuzabadi**[1]

Received: 11 May 2019 / Accepted: 3 August 2019

Abstract

The immobilization of a copper complex by covalent anchoring of 2-hydroxybenzophenone on the surface of amine-functionalized magnetic nanoparticles was reported. The structure and morphology of the catalyst was characterized by different techniques such as Fourier-transform infrared spectroscopy (FT-IR), X-ray diffraction (XRD), transmission electron micrograph (TEM), scanning electron microscopy (SEM), energy dispersive X-ray spectroscopy (EDS), vibrating sample magnetometer (VSM) and inductively coupled plasma (ICP) spectroscopy. This efficient and cost effective catalyst was applied in the N-arylation reaction and the products were obtained in good to excellent yields in short reaction times. The cost-effective catalyst demonstrated high stability, which could be facilely separated from the reaction mixture by applying an external magnet and recycled at least four times with only a slight decrease in its activity.

Graphic Abstract

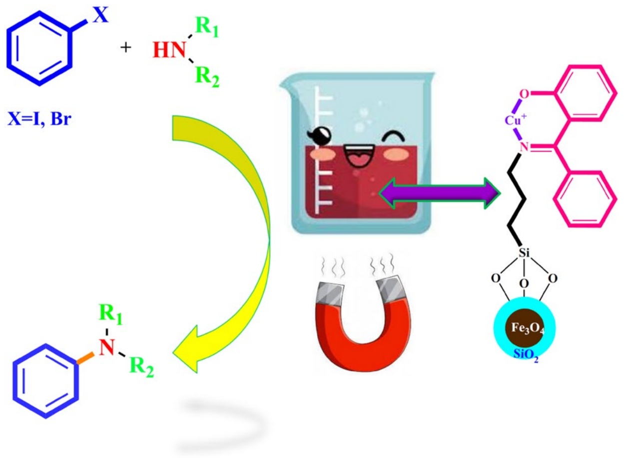

Keywords Heterogeneous · Magnetic materials · Catalytic properties · NFG-arylation reaction

1 Introduction

The N-arylation coupling reaction is the most powerful and widely used method for the construction of C–N bond which is one of the most important areas of research in synthetic organic chemistry [1]. The N-aryl nitrogen heterocycles are unique building blocks in numerous biologically important natural compounds [2–5] pharmaceuticals [6–9] and industrial applications [10].

Electronic supplementary material The online version of this article (https://doi.org/10.1007/s10562-019-02929-x) contains supplementary material, which is available to authorized users.

✉ Zahra Asadi
zasadi@shirazu.ac.ir

[1] Department of Chemistry, College of Sciences, Shiraz University, Shiraz 71454, Iran

Recently, remarkable improvement has been made on the transition-metal-catalyzed N-arylation reaction. These researches have particularly focused on Cu-promoted Ullmann [11–16] or Pd-mediated Buchwald-Hartwig coupling reactions [17–22]. Due to the high cost of palladium, less costly metals become more desirable. Since copper is an inexpensive and available metal, its use is highly demanded to develop new catalyst systems [23]. However, in order to promote N-arylation reaction by Cu catalysts, often high temperature (125–220 °C) and large amounts of catalyst are required [24]. Consequently, by using suitable bidentate chelating ligands such as N,N-, O,O-, and N,O-chelators, the reaction outcome can be improved [25, 26]. On the other hand many catalysts used in N-arylation reaction are homogeneous that suffer from drawbacks associated with the separation and recovery of the catalysts. To solve these problems, homogeneous catalysts are typically immobilized on various insoluble supports, rendering them heterogeneous in nature [27–33]. The efficiency of heterogeneous catalyst systems can be improved by using nanosized catalysts because of their small size and high surface area. However, the supporting nanocatalysts such as TiO_2 nanoparticles [34], ionic liquids [35], carbon nanotubes [36], SBA-15 [37], MCM-41 [38, 39] or some polymers [40] have disadvantages such as tedious workup processes, difficult and expensive separation of catalyst from the reaction mixture. Moreover, some of these supports need high temperature for calcination or time consuming and boring conditions for their preparation. Thus, the use of magnetic nanoparticles (MNPs) as a catalyst support appears to be the most logical solution: their insoluble and superparamagnetic nature enables simple and efficient separation of the catalysts from the reaction mixture with the help of an external magnet [41–43].

In continuing our efforts to develop economical and eco-friendly synthetic pathways for coupling reactions [44–46], in the present work, we would like to introduce a new heterogeneous magnetic reusable catalyst supported imine copper complex for the N-arylation reaction. This system is of interest as it possesses several advantages, such as short reaction time, high yields, simple separation and reusability of the catalyst.

2 Experimental

2.1 Synthesis of Fe_3O_4

Fe_3O_4 magnetic nanoparticles (MNPs) were synthesized according to a previously reported method [47]. 3.0 g $FeCl_3·6H_2O$ and 2.1 g $FeCl_2·4H_2O$ were added to 500 mL deionized water and stirred under the continuous flow of nitrogen at 83 °C. Then, sodium hydroxide (10 wt%) was added dropwisely to the solution until the pH value reached to 12. The reaction temperature was reduced and kept at 63 °C for 1 h. The black solid product was isolated by external magnet, washed with distilled water and ethanol for several times and dried in the vacuum.

2.2 Synthesis of Fe_3O_4@SiO_2 Core–Shell Microspheres

2.0 g Fe_3O_4 nanoparticles were suspended in 70 mL ethanol and 10 mL distilled water by sonication for 25 min. Then, 5 mL of aqueous solution of ammonia ($NH_3·H_2O$, 25%) and 4 mL of tetraethylorthosilicate (TEOS) were slowly added and the mixture stirred for further 24 h. The coated NPs were magnetically collected and rinsed with ethanol and deionized water, respectively.

2.3 Synthesis of Amine Functionalized Fe_3O_4@SiO_2 (AS-MNPs)

The Fe_3O_4@SiO_2 (1.0 g) was dispersed in dry toluene (50 mL) with ultrasonicating for 30 min. To the resulting suspension, 1.5 mL of (3-aminopropyl)triethoxysilane (APTES) was added and the mixture was refluxed for 24 h under N_2 atmosphere. The mixture was subjected to magnetic decantation and the obtained solid was washed with toluene and ethanol for several times.

2.4 Immobilization of Schiff Base Ligand on AS-MNPs (HB@AS-MNPs)

1.0 g of AS-MNPs and an ethanolic solution (30 mL) of 2-hydroxybenzophenone (2.0 mmol, 0.4 g) was refluxed overnight under N_2 atmosphere. The solid product was separated magnetically, washed with ethanol and dried under vacuum.

2.5 Synthesis of Cu-HB@AS-MNPs Catalyst

1.0 g of as-synthesized HB@AS-MNPs was dispersed in 40 mL absolute ethanol, followed by the addition of copper(II) acetate. The mixture was stirred under reflux for 24 h under an inert (N_2) atmosphere. The catalyst was collected by a magnetic bar and washed three times with ethanol. The Cu-HB@AS-MNPs catalyst was obtained with loading of 1.48 mmol of Cu per gram determined by ICP.

2.6 General Procedure for N-arylation Reaction Catalyzed by Cu-Catalyst

Amine (1.0 mmol) was added to a suspension of aryl halide (1.0 mmol), K_2CO_3 (2.0 mmol), and Cu catalyst (0.047 g, 7 mol%) in DMSO (3.0 mL) in a 10 mL reaction flask. The reaction mixture was stirred at 130 °C and monitored by

TLC to determine completion of the reaction. Subsequently, the catalyst was separated magnetically and the reaction mixture was diluted with ethyl acetate (20 mL). The solvent was evaporated under reduced pressure to get the crude product and the product was purified by column chromatography on silica using *n*-hexane and ethyl acetate.

3 Results and Discussion

3.1 Characterization of Cu-HB@AS-MNPs Catalyst

The process for the preparation of Cu-HB@AS-MNPs catalyst is shown in Scheme 1. Fe_3O_4 particles were synthesized by the co-precipitation of Fe^{3+} and Fe^{2+} salt and coated with a thin layer of silica using a sol–gel process to give $Fe_3O_4@SiO_2$. The resulting silica-coated MNPs were then modified with (3-aminopropyl) triethoxysilane (APTES) to obtain amine functionalized MNPs (AS-MNPs). Subsequently, AS-MNPs was reacted with 2-hydroxybenzophenone in ethanol to afford HB@AS-MNPs. Finally, HB@AS-MNPs was treated with copper(II) acetate in ethanol to afford the desired Cu-HB@AS-MNPs catalyst. The catalyst was characterized by SEM, TEM, EDX, CHN, FT-IR, ICP, XRD and VSM.

The size and morphology of the synthesized catalyst were characterized using TEM and SEM. The TEM images displayed a dark Fe_3O_4 core surrounded by a gray silica shell with a thickness of about 4 nm (Fig. 1a). SEM image indicated that the synthesized Cu-HB@AS-MNPs had uniformity and a spherical morphology (Fig. 1b). The average size of the catalyst particles was 15 nm. In order to verify the existence of all expected elements in the Cu-HB@AS-MNPs catalyst EDX analysis was employed. The results confirmed the attachment of copper complex on the surface of MNPs and the components of the catalyst were Fe, Si, N, C, O and Cu elements (Fig. 1c). The exact quantity of copper loaded on the Cu-HB@AS-MNPs catalyst was measured using ICP. The ICP analysis of the catalyst indicated that 1.48 mmol/g of copper was loaded onto the nanomagnetic catalyst.

Successful functionalization of the MNPs can be determined from the FT-IR spectroscopic technique. The FT-IR spectra of Fe_3O_4, $Fe_3O_4@SiO_2$, AS-MNPs, HB@AS-MNPs and Cu-HB@AS-MNPs catalyst are exhibited in Fig. 2. The IR spectra of bare Fe_3O_4 (Fig. 2a) illustrated the absorption band at 590 cm^{-1} attributed to Fe–O bond vibration [48, 49] and a broad band at 3452 cm^{-1} assigned to the presence of OH groups on the surface of the MNPs [50]. FT-IR spectra of $Fe_3O_4@SiO_2$ (Fig. 2b) showed specific peaks for Si–O–Si bond at 1087 cm^{-1} and 790 cm^{-1}, which confirmed the presence of silica phase [51]. In the FT-IR spectra of AS-MNPs (Fig. 2c), additional peaks due to N–H stretching vibration and NH_2 bending mode of free NH_2 group were seen at 3481 and 1677 cm^{-1}, respectively [52, 53]. Furthermore, the absorption band corresponding to C-H band of propyl group from APTES was appeared at 2985 and 2862 cm^{-1} [54, 55]. In Fig. 2d, a characteristic peak at 1670 cm^{-1} was related to C=N stretching vibrations of HB@AS-MNPs, which affirmed that 2-hydroxybenzophenone was successfully immobilized on the surface of functionalized silica [56, 57]. In the FT-IR spectrum of Cu-HB@AS-MNPs (Fig. 2e), due to

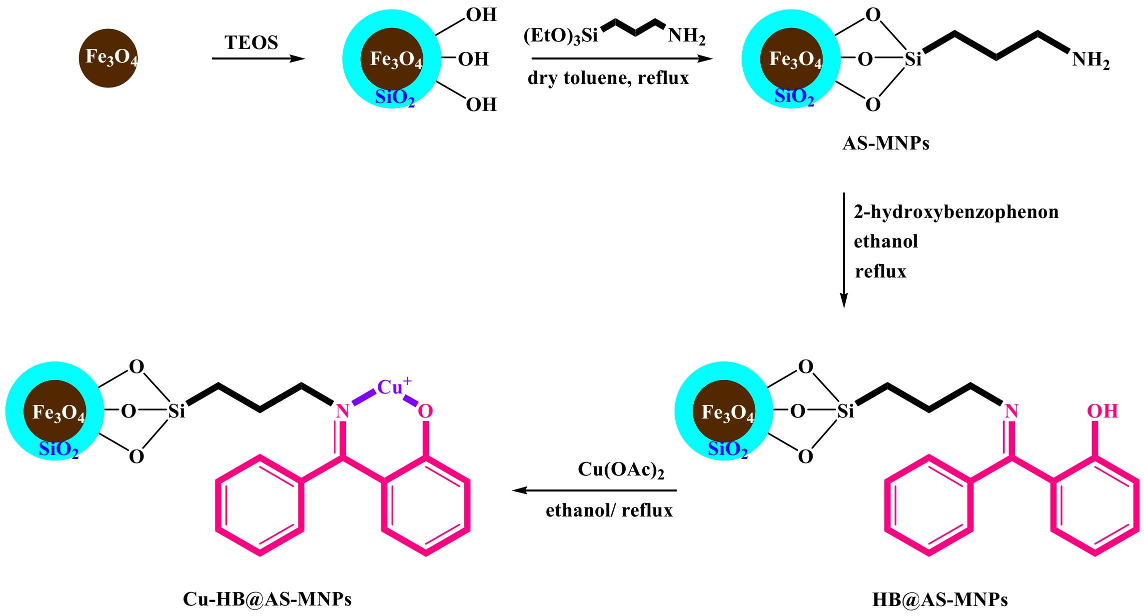

Scheme 1 A schematic illustration for the synthesis of Cu-HB@AS-MNPs catalyst

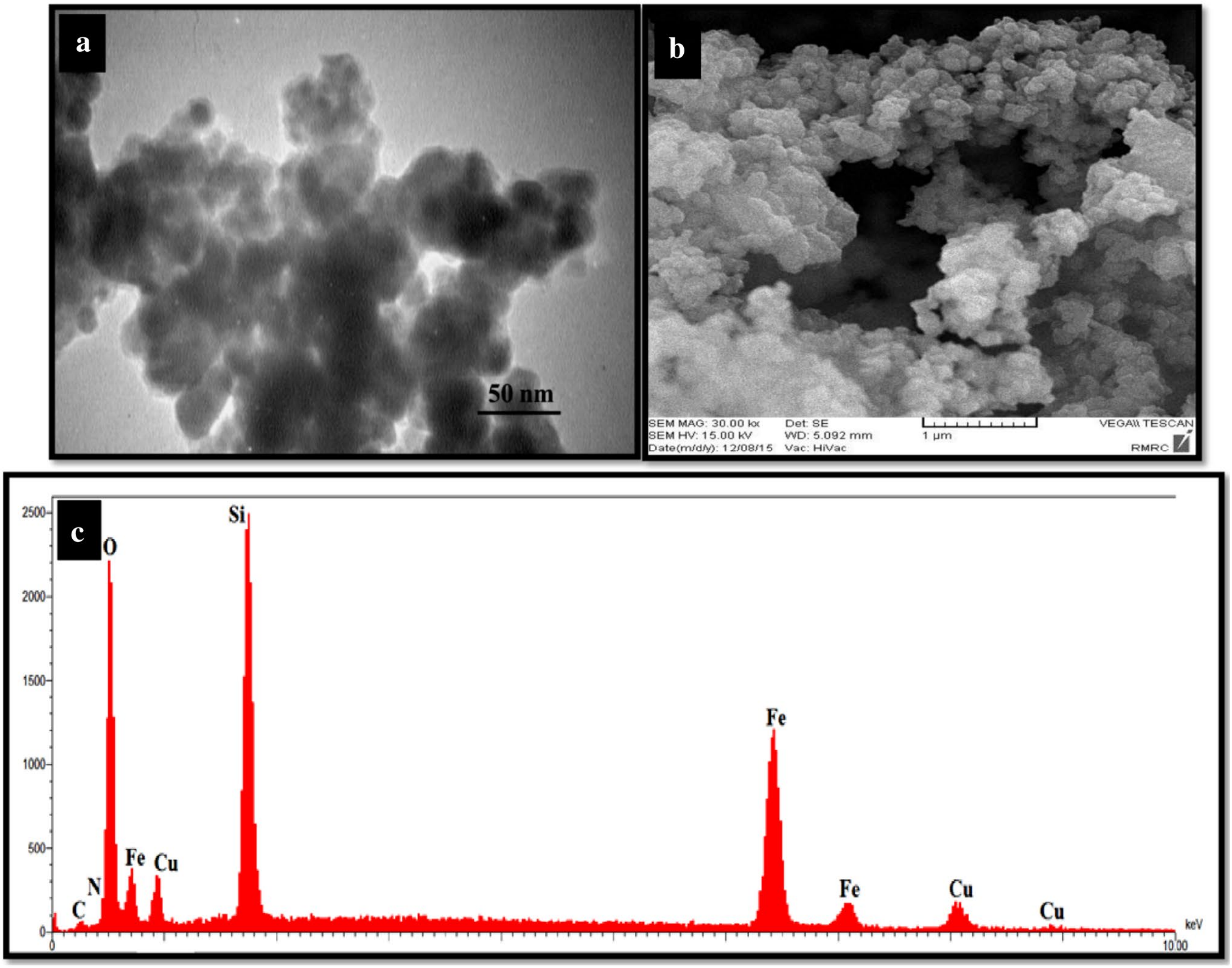

Fig. 1 TEM (**a**), SEM (**b**), and EDX pattern of Cu-HB@AS-MNPs catalyst (**c**)

the binding of azomethine nitrogens to the metal ion, the absorption peak of C=N was shifted to a lower frequency at 1636 cm^{-1}.

To investigate the composition and crystallinity of HB@AS-MNPs and Cu-HB@AS-MNPs; XRD technique was used. As shown in Fig. 3a, b the position and relative intensities of all peaks in the XRD pattern of MNPs were in good conformity with the face centered cubic (fcc) Fe_3O_4, indicating retention of the crystalline structure during functionalization of MNPs. The MNPs demonstrated six characteristic diffraction peaks at $2\theta = 30.3°$, 35.6°, 43.2°, 53.1°, 57.2°, and 63.0° due to (220), (311), (400), (422), (511) and (440), respectively [58, 59].

Furthermore, a broad peak at $2\theta < 20$ was assigned to amorphous state SiO_2 shells [60]. By adding $Cu(OAc)_2$ to HB@AS-MNPs, these characteristic peaks appeared with negligible shifts. The sharp peaks of HB@AS-MNPs did not change in the XRD pattern of Cu-HB@AS-MNPs catalyst, confirming that the structure of the catalyst did not deform after metalation (Fig. 3b).

Magnetization properties of HB@AS-MNPs and Cu-HB@AS-MNPs were investigated by VSM in the employed magnetic field from − 8500 to +8500 Oe. The magnetization curves indicated that both HB@AS-MNPs and Cu-HB@AS-MNPs were superparamagnetic at room temperature and could be efficiently separated from the reaction mixture using an external magnet (Fig. 4a, b). The saturation magnetization of HB@AS-MNPs and Cu-HB@AS-MNPs were 46 and 33 emu g^{-1}, respectively. The decrease in the magnetization value of Cu-HB@AS-MNPs indicated the successful attachment of Cu on the surface of HB@AS-MNPs.

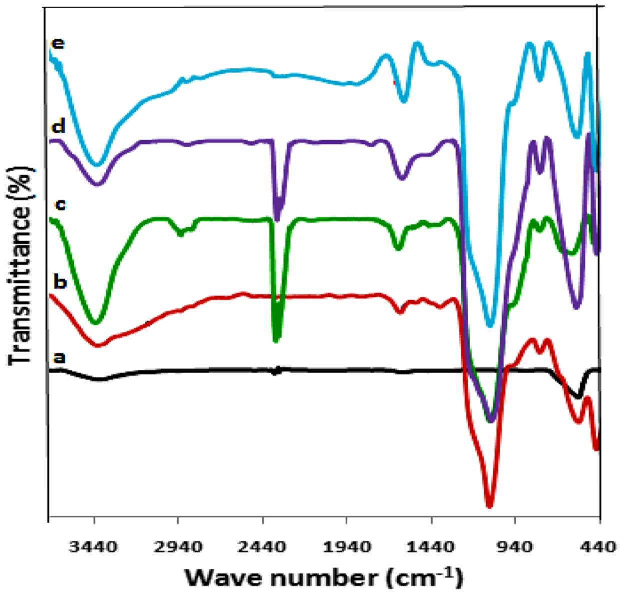

Fig. 2 FT-IR spectra of Fe_3O_4 (a), Fe_3O_4@SiO_2 (b), AS-MNPs (c), HB@AS-MNPs (d), and Cu-HB@AS-MNPs catalyst (e)

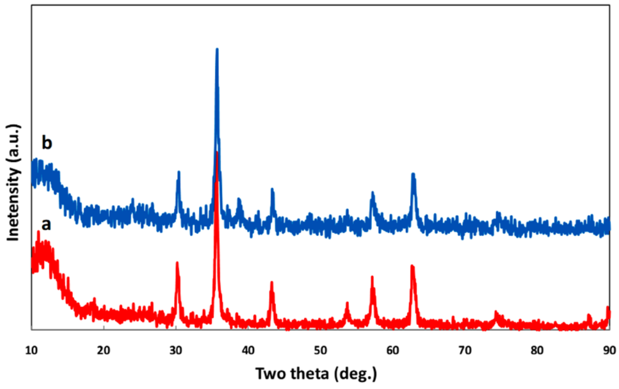

Fig. 3 XRD patterns of HB@AS-MNPs (a) and Cu-HB@AS-MNPs catalyst (b)

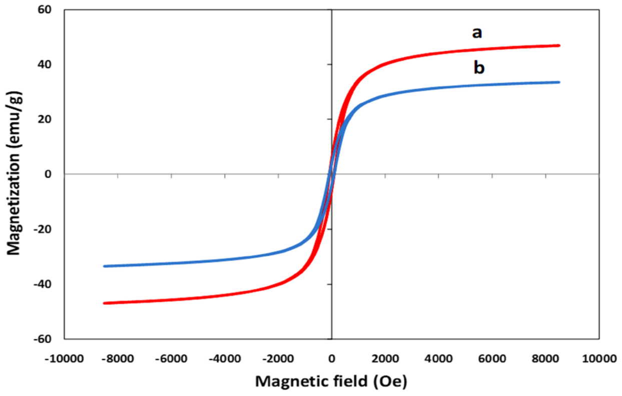

Fig. 4 VSM curves of HB@AS-MNPs (a) and Cu-HB@AS-MNPs (b)

3.2 N-arylation of Amines with Aryl Halides Catalyzed by Cu-HB@AS-MNPs

To evaluate the applicability of Cu-HB@AS-MNPs catalyst in the N-arylation reaction, the reaction conditions were surveyed by using iodobenzene and benzimidazole (2a) as model substrates. The initial attempt was focused on the coupling reaction of 2a (1.0 mmol) with iodobenzene (1.0 mmol) using 10 mol% of Cu catalyst in DMF at 135 °C (Table 1, entry 1), and the desired N-arylated product was obtained 92% of the yield. Then, different parameters such as solvent, base, temperature and catalyst amount were examined to obtain the optimal reaction conditions. The influence of the solvent on the reaction was investigated and good yield was obtained with DMF and DMSO (Table 1, entries 1, 2). In order to increase the sustainability of the method and owing to the awful environmental effect of DMF, DMSO was chosen as the most suitable solvent. Other solvents such as, DMA, PEG and H_2O/TBAB (tetrabutyl ammonium bromide, as a surfactant) were found to be inferior (Table 1, entries 3–5). Moreover, in the absence of solvent, 70% yield of product was observed (Table 1, entry 6). We also screened the use of various bases such as K_2CO_3, CH_3COONa, KOH and ^{t}BuOK (Table 1, entry 2, entries 7–9) and the results clearly indicated that K_2CO_3 was the best one (Table 1, entry 2).Three different catalyst amounts were tested. By using 5 mol% and 7 mol% of Cu-catalyst, 80% and 90% of products were obtained, respectively (Table 1, entries 10, 11). Since the yield of the product did not change remarkably upon decreasing the catalyst amount from 10 to 7 mol%, 7 mol% of Cu-catalyst was chosen as the catalyst amount. It should be noted that no coupling product was observed in the absence of the Cu catalyst, confirming the necessity of using the Cu-HB@AS-MNPs as catalyst for the N-arylation reaction (Table 1, entry 12). Also, some tests were carried out at several temperatures and it was found that by increasing the temperature from 100 to 130 °C, the yield increased from 60 to 90% (Table 1, entries 13–15). However, at 140 °C no significant reaction progress compared to 130 °C was observed (Table 1, entry 16). Therefore, 130 °C is a suitable temperature to push this reaction forward (Table 1, entry 15). As a result the entry 15 of Table 1 was selected as optimized conditions for N-arylation reaction using Cu-HB@AS-MNPs catalyst.

Having the optimized reaction conditions in hand, the scope of this reaction with various functionalized iodobenzenes and amines was explored (Scheme 2). As shown in Scheme 2, the coupling reactions were accomplished with high to excellent yields (80–95%). The N-arylation reaction was efficiently promoted for aryl iodides with benzimidazole to give the corresponding coupling products up to 92% yield (Fig. 3a–c). Good yield of product was obtained for bromobenzene in longer time (Fig. 3a). Extending this

Table 1 Optimization of the N-arylation reaction between iodobenzene (1.0 mmol) and benzimidazole catalyzed by Cu-HB@AS-MNPs catalyst

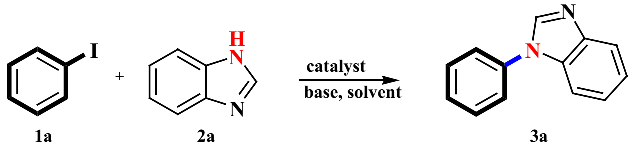

Entry	Solvent	Catalyst amount (mol%)	Bases	Temperature (℃)	Yield (%)[a]
1	DMF	10	K_2CO_3	130 °C	92
2	DMSO	10	K_2CO_3	130 °C	90
3	DMA	10	K_2CO_3	130 °C	60
4	PEG(200)	10	K_2CO_3	130 °C	60
5	H_2O/TBAB	10	K_2CO_3	Reflux	75[b]
6	None	10	K_2CO_3	130 °C	70
7	DMSO	10	CH_3COONa	130 °C	30
8	DMSO	10	KOH	130 °C	40
9	DMSO	10	^{t}BuOK	130 °C	60
10	DMSO	5	K_2CO_3	130 °C	80
11	DMSO	7	K_2CO_3	130 °C	90
12	DMSO	–	K_2CO_3	130 °C	–
13	DMSO	7	K_2CO_3	100 °C	60
14	DMSO	7	K_2CO_3	115 °C	70
15	DMSO	7	K_2CO_3	130 °C	90[c]
16	DMSO	7	K_2CO_3	140 °C	92

Reaction conditions: iodobenzene (1.0 mmol), benzimidazole (1.0 mmol), base (2.0 mmol), solvent (3.0 mL), Cu-HB@AS-MNPs (7 mol%, 0.047 g), 130 °C, 4 h

[a] Isolated yields

[b] 2.0 mmol of TBAB was used

[c] The optimum conditions for N-arylation reaction

chemistry to include pyrazole as substrate was also quite successful. The reaction of pyrazole with aryl halides led to the synthesis of products containing the biological active fragments (Fig. 3d–f). In the reaction of benzimidazole and pyrazole with substituted iodobenzene, electron-donating group (CH_3) on the aryl halide depressed the efficiency of the reactions to some extent (Fig. 3c, f). However, electron-withdrawing aryl halide (1-iodo-4-nitrobenzene) underwent in the coupling reactions well to afford the products in higher yields (Fig. 3b, e, h). In addition, hydrazobenzene reacted with iodobenzene and 4-nitroiodobenzene to give new symmetrical products in high yields (Fig. 3g, h). The optimized reaction conditions were also applied to the cross coupling of diphenylcarbazide with iodobenzene and a new product containing four functional groups was synthesized (Fig. 3i). The products were characterized by ^{1}H NMR.

Moreover, the reusability of Cu-HB@AS-MNPs catalyst was examined due to the potential benefits in commercial applications. In this regard, the reaction of iodobenzene with benzimidazole was chosen as the model reaction. After completion of the reaction, the catalyst was separated magnetically, successively washed with deionized water, ethanol and ethyl acetate and reused four times under the same reaction conditions. As shown in Fig. 5 only a slight decreasing in the catalytic activity was observed after each run. The FT-IR spectra of the reused catalyst (Fig. 6) confirmed that the structure of the catalyst was remained unchanged after recovery.

After four runs in N-arylation reaction, the TEM image demonstrated that the morphology and the size of the recovered catalyst was almost the same as that of freshly prepared catalyst (Fig. 7).

On the basis of these experiments, in can be concluded that the Cu-HB@AS-MNPs catalyst was stable and heterogeneous in practice.

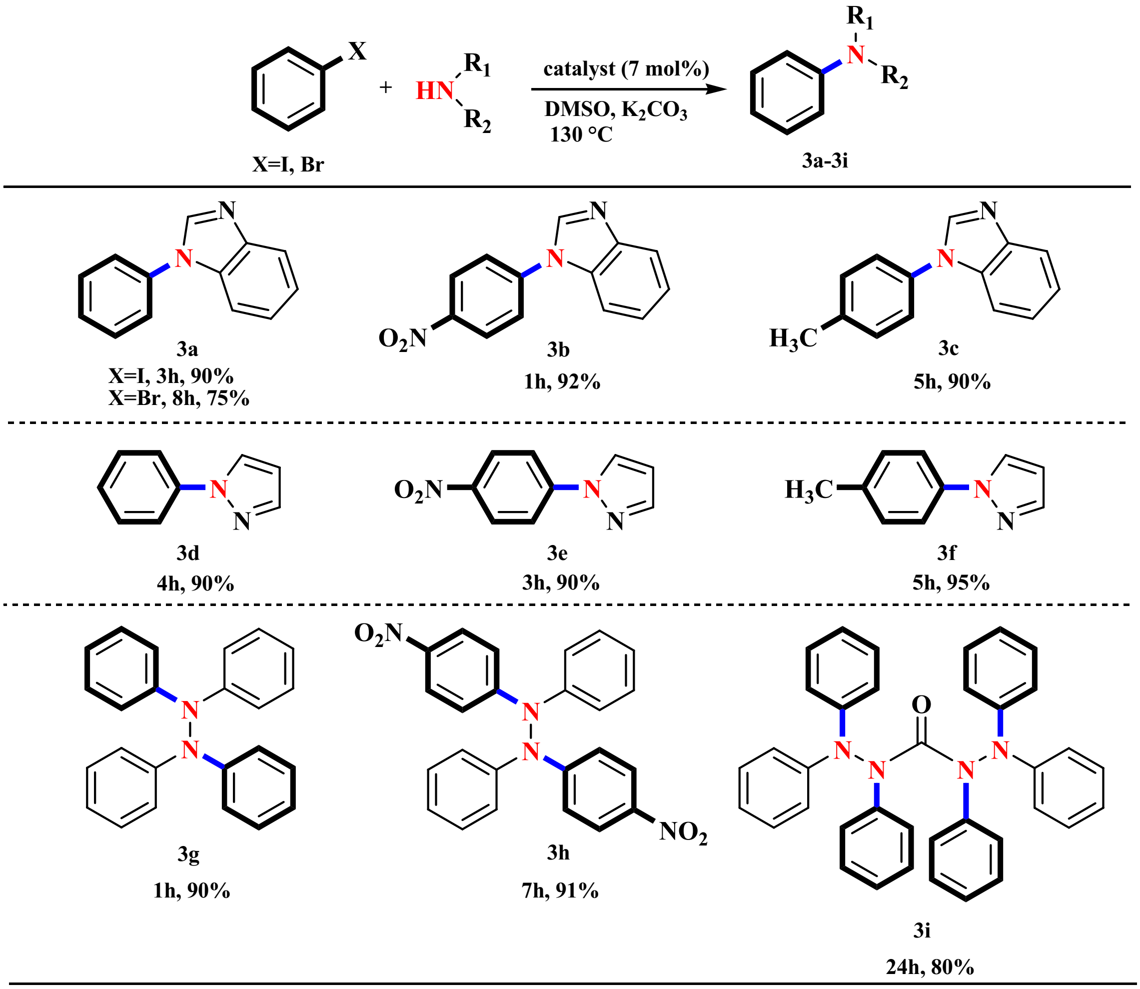

Scheme 2 Summary of the N-arylation reaction of aryl iodides with amines under the optimized conditions. Reaction conditions: aryl iodide (1.0 mmol), amines (1.0 mmol), base (2.0 mmol), solvent (3.0 mL), Cu-HB@AS-MNPs (7 mol%, 0.047 g), 130 °C

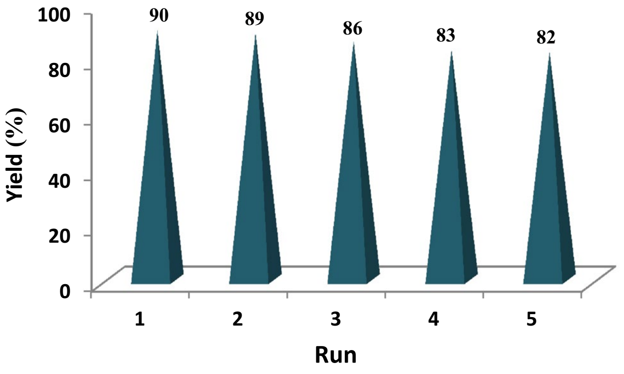

Fig. 5 The reusability of the Cu-HB@AS-MNPs for reaction between benzimidazole and iodobenzene under the optimized conditions

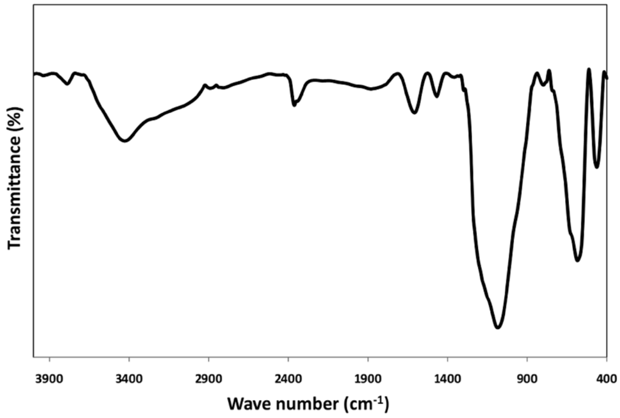

Fig. 6 FT-IR spectra of the Cu-HB@AS-MNPs catalyst after five runs

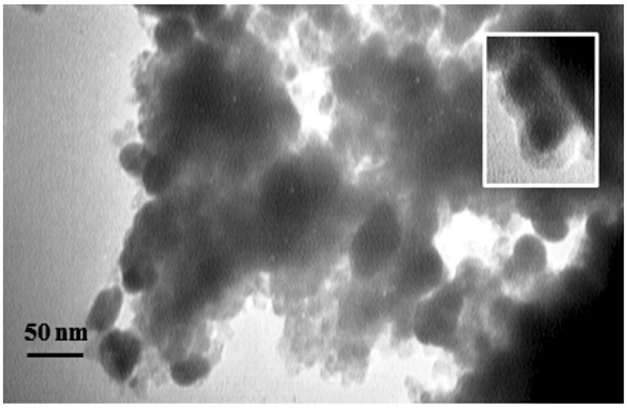

Fig. 7 TEM image of Cu-HB@AS-MNPs catalyst after four cycles in the N-arylation reaction of iodobenzene with benzimidazole

4 Conclusion

In summary, we have prepared a retrievable and sustainable nano magnetic catalyst (Cu-HB@AS-MNPs) used for a variety of organic transformations such as N-arylation reaction in good to excellent yields. In order to decrease the harmful effect of toxic solvents, DMSO with low toxicity was chosen as the solvent of this reaction. The attractive features of this catalyst compared to other reported catalysts are the use of low cost metal center, high yield, short reaction time for completion of the reaction and recyclability that makes the catalyst efficient after four cycles. Notably, magnetic separation/re-dispersion strategy, cause this catalyst to be a good candidate for the goal of green chemistry.

Acknowledgements Support of this paper by Shiraz University is gratefully acknowledged.

References

1. Baig RBN, Nadagouda MN, Varma RS (2014) Green Chem 16:4333
2. Hili R, Yudin AK (2006) Nat Chem Biol 2:284
3. Baig RBN, Varma RS (2013) Green Chem 15:398
4. Corbet J-P, Mignani G (2006) Chem Rev 106:2651
5. Evano G, Blanchard N, Toumi M (2008) Chem Rev 108:3054
6. Surry DS, Buchwald SL (2011) Chem Sci 2:27
7. Liao X, Weng Z, Hartwig JF (2008) J Am Chem Soc 130:195
8. Monnier F, Taillefer M (2009) Angew Chem Int Ed 48:6954
9. Shen Q, Hartwig JF (2007) J Am Chem Soc 129:7734
10. Prabakaran K, Manivel P, Khan FN (2010) Tetrahedron Lett 51:4340
11. Sambiagio C, Marsden SP, Blacker AJ, McGowan PC (2014) Chem Soc Rev 43:3525
12. Huang P-C, Gandeepan P, Cheng C-H (2013) Chem Commun 49:8540
13. Masters KS, Rauws TR, Yadav AK, Herrebout WA, Van der Veken B, Maes BU (2011) Chem Eur J 17:6315
14. Li Q, Huang Y, Chen T, Zhou Y, Xu Q, Yin S-F, Han L-B (2014) Org Lett 16:3672
15. Li X, He L, Chen H, Wu W, Jiang H (2013) J Org Chem 78:3636
16. Reddy AS, Reddy KR, Rao DN, Jaladanki CK, Bharatam PV, Lam PY, Das P (2017) Org Biomol Chem 15:801
17. Alamdari RF, Haqiqi MG, Zekri N (2016) New J Chem 40:1287
18. Yugandar S, Konda S, Ila H (2016) J Org Chem 81:2035
19. Youn SW, Bihn JH, Kim BS (2011) Org Lett 13:3738
20. Kumar RK, Punniyamurthy T (2012) RSC Adv 2:4616
21. Haffemayer B, Gulias M, Gaunt MJ (2011) Chem Sci 2:312
22. Yang D, Burugupalli S, Daniel D, Chen Y (2012) J Org Chem 77:4466
23. Iranpoor N, Panahi F, Roozbin F, Rahimi S, Haghighi MG (2017) Mol Catal 438:214
24. Sueki S, Kuninobu Y (2013) Org Lett 15:1544
25. Zhang Q, Wang D, Wang X, Ding K (2009) J Org Chem 74:7187
26. Ullmann F (1903) Ber Dtsch Chem Ges 36:2382
27. Rajabi F, Schaffner D, Follmann S, Wilhelm C, Ernst S, Thiel WR (2015) ChemCatChem 7:3513
28. Schätz A, Long TR, Grass RN, Stark WJ, Hanson PR, Reiser O (2010) Adv Funct Mater 20:4323
29. Sharma RK, Dutta S, Sharma S, Zboril R, Varma RS, Gawande MB (2016) Green Chem 18:3184
30. Yang W, Wei L, Yan T, Cai M (2017) Catal Sci Technol 7:1744
31. Almeida TSD, Guima K-E, Silveira RM, da Silva GC, Martines MAU, Martins CA (2017) RSC Adv 7:12006
32. Molnár Á (2011) Chem Rev 111:2251
33. Polshettiwar V, Luque R, Fihri A, Zhu H, Bouhrara M, Basset J-M (2011) Chem Rev 111:3036
34. Soni SS, Kotadia DA (2014) Catal Sci Technol 4:510
35. Karimi B, Tavakolian M, Akbari M, Mansouri F (2018) ChemCatChem 10:3173
36. Melchionna M, Marchesan S, Prato M, Fornasiero P (2015) Catal Sci Technol 5:3859
37. Nasrollahzadeh M, Sajadi SM, Maham M (2015) J Mol Catal A 396:297
38. Nikoorazm M, Ghorbani-Choghamarani A, Noori N (2015) Appl Organomet Chem 29:328
39. Ghorbani-Choghamarani A, Nikpour F, Ghorbani F, Havasi F (2015) RSC Adv 5:33212
40. Shao L, Qi C, Zhang X-M (2014) RSC Adv 4:53105
41. Chouhan G, Wang D, Alper H (2007) Chem Commun. https://doi.org/10.1039/B711298J
42. Phan NTS, Jones CW (2006) J Mol Catal A 253:123
43. Miraki MK, Arefi M, Salamatmanesh A, Yazdani E, Heydari A (2018) Catal Lett 148:3378
44. Mandegani Z, Asadi M, Asadi Z, Mohajeri A, Iranpoor N, Omidvar A (2015) Green Chem 17:3326
45. Firuzabadi FD, Asadi Z, Panahi F (2016) RSC Adv 6:101061
46. Firuzabadi FD, Asadi Z (2018) ChemistrySelect 3:9857
47. Baig RBN, Varma RS (2012) Chem Commun 48:6220
48. Salamatmanesh A, Miraki MK, Yazdani E, Heydari A (2018) Catal Lett 148:3257
49. Liu Y, Wang X, Chen C, Li L, Yu H, Wu Q, Xie C, Yu S, Liu S (2018) Catal Lett 148:3147
50. Chinchole AN, Dubey AV, Kumar AV (2019) Catal Lett 149:1224
51. Tukhani M, Panahi F, Khalafi-Nezhad A (2018) ACS Sustain Chem Eng 6:1456
52. Sobhani S, Vahidi Z, Zeraatkar Z, Khodadadi S (2015) RSC Adv 5:36552
53. Esmaeilpour M, Javidi J, Nowroozi Dodeji F, Mokhtari Abarghoui M (2014) J Mol Catal A 393:18
54. Wang P, Zhu H, Liu M, Niu J, Yuan B, Li R, Ma J (2014) RSC Adv 4:28922
55. Keyhaniyan M, Shiri A, Eshghi H, Khojastehnezhad A (2018) Appl Organomet Chem 32:e4344

56. Asadi Z, Asadi M, Firuzabadi FD, Shorkaei MR (2014) J Ind Eng Chem 20:4227
57. Esmaeilpour M, Sardarian AR, Javidi J (2014) J Organomet Chem 749:233
58. Wei X, Wan X, Miao J, Zhang R, Zhang J, Niu QJ (2019) Catal Lett 149:823
59. Maleki A, Kari T (2018) Catal Lett 148:2929
60. Sharma RK, Yadav M, Gaur R, Monga Y, Adholeya A (2015) Catal Sci Technol 5:2728